

Onset of thermal convection in a horizontal layer of granular gas

Evgeniy Khain and Baruch Meerson

Racah Institute of Physics, Hebrew University of Jerusalem, Jerusalem 91904, Israel

The Navier-Stokes granular hydrodynamics is employed for determining the threshold of thermal convection in an infinite horizontal layer of granular gas. The dependence of the convection threshold, in terms of the inelasticity of particle collisions, on the Froude and Knudsen numbers is found. The morphology of convection cells at the onset is determined. At large Froude numbers, the Froude number drops out from the problem. As the Froude number goes to zero, the convection instability turns into a recently discovered phase separation instability.

PACS numbers: 45.70.Qj

Introduction. Fluidized granular medium exhibits a plethora of fascinating pattern-formation phenomena that have been a subject of much recent interest [1]. In this work we address thermal (buoyancy-driven) granular convection [2, 3, 4, 5, 6]. Being unrelated to the shear or time-dependence introduced by the system boundaries, it resembles the Rayleigh-Bénard convection in classical fluid [7] and its compressible modifications [8, 9, 10, 11]. In classical fluid the convection is driven by an externally imposed negative temperature gradient. In a fluidized granular medium a negative temperature gradient sets in spontaneously because of the energy loss by inelastic collisions. In the simplest model of inelastic hard spheres, the convection sets in when the inelasticity coefficient $q = (1 - r) = 2$ exceeds a critical value (r is the coefficient of normal restitution) [2]. Thermal convection was first observed in molecular dynamics (MD) simulations of granular gas in a two-dimensional (2D) square box [2]. The boundaries of the box did not introduce any shear or time-dependence: the system was driven by a stress-free thermalizing base. Experiment with a highly fluidized three-dimensional granular flow [3] gives strong evidence for thermal convection, though energy loss at the side walls introduces complications [3, 6]. A clear identification of thermal convection in experiment requires a large aspect ratio in the horizontal direction, so that multiple convection cells can be observed. MD simulations of a large-aspect-ratio system in 2D indeed showed multiple convection cells [4].

Recently a continuum theory of thermal granular convection has been formulated [5] in the framework of the Navier-Stokes granular hydrodynamics [12]. In the dilute limit, the hydrodynamics is systematically derivable from kinetic equations [13]. It demands nearly elastic collisions, $q \rightarrow 1$, and small Knudsen numbers for its validity. The set of hydrodynamic equations was solved numerically in 2D [5]. It was observed that the transition to convection occurs via a supercritical bifurcation, the inelasticity q being the control parameter, in agreement with MD simulations [2]. The present work employs the hydrodynamic formulation [5] to perform the linear stability analysis of the static state. We determine the

convection threshold as a function of the scaled parameters of the problem and of the horizontal wave number of small perturbations. This makes it possible to predict the convection threshold and determine the morphology of the convection cells in an infinite horizontal layer, a standard setting for convection in classical fluids [7, 14]. In the limit of zero gravity we establish a connection between the thermal convection and phase-separation instability [15, 16, 17, 18, 19, 20].

Model and static state. Let a big number of identical smooth hard spheres with diameter d and mass m move and inelastically collide inside an infinite horizontal layer with height H . The gravity acceleration g is in the negative y direction. The system is driven by a rapidly vibrating base. We shall model it by prescribing a constant temperature T_0 at $y = 0$. The top wall is assumed elastic. Hydrodynamics deals with coarse-grained fields: the number density of grains $n(r;t)$, granular temperature $T(r;t)$ and mean flow velocity $v(r;t)$. In the dilute limit, the scaled governing equations are [5]:

$$dn/dt + n \nabla \cdot v = 0; \quad (1)$$

$$n dv/dt = -\nabla \cdot P - F \eta_y \epsilon \quad (2)$$

$$n dT/dt + n T \nabla \cdot v = K r^{-1} \nabla^2 (T r) - K R n^2 T^{3-2}; \quad (3)$$

Here $d/dt = \partial/\partial t + v \cdot \nabla$ is the total derivative, $P = -n T I + (1-2) K T^{1-2} \hat{D}$ is the stress tensor, $D = (1/2) (\nabla v + (\nabla v)^T)$ is the rate of deformation tensor, $\hat{D} = D - (1/2) \text{tr}(D) I$ is the deviatoric part of D , and I is the identity tensor. In the dilute limit, the bulk viscosity of the gas is negligible compared to the shear viscosity [12], so only the shear viscosity is taken into account. In addition, we have neglected the small viscous heating term in the heat balance equation (3). In the 2D geometry, the three scaled parameters entering Eqs. (2) and (3) are the Froude number $F = m g H = T_0$, the Knudsen number $K = 2^{1-2} (dH/n_i)^{-1}$ and the relative heat loss parameter $R = 8qK^{-2}$. Furthermore, n_i is the number of particles per unit length in the horizontal direction, divided by the layer height H . It will be convenient to

use the relative heat loss number R instead of q . In Eqs. (1)–(3), the distance is measured in the units of H , the time in units of $H = T_0^{1=2}$, the density in units of ρ_0 , the temperature in units of T_0 , and the velocity in units of $T_0^{1=2}$.

The boundary conditions (BCs) for the temperature are $T(x; y = 0; t) = 1$ and zero normal component of the heat flux at the upper wall: $\partial T = \partial y(x; y = 1; t) = 0$. For velocities we demand zero normal components and slip conditions at the boundaries. The total number of particles in the system is conserved:

$$\lim_{L \rightarrow 1} \frac{1}{2L} \int_{-L}^L dx \int_{-L}^L dy n(x; y; t) = 1; \quad (4)$$

where we have introduced the horizontal dimension $2L$. The hydrodynamic problem is characterized by the three scaled numbers F , K and R .

The simplest steady state of the system is static: no mean flow. At a nonzero gravity the density n_s and temperature T_s of the static state depend only on y , and are described by the equations

$$(n_s T_s)' + F n_s = 0 \quad \text{and} \quad (T_s^{1=2} T_s^0)' - R T_s^2 T_s^{3=2} = 0; \quad (5)$$

where the primes denote the y -derivatives. The BCs are $T_s(0) = 1$ and $T_s'(1) = 0$, the normalization condition is $\int_{-1}^1 dy n_s(y) = 1$. The static state (see Fig. 1) is characterized by two scaled numbers: F and R , and can be found analytically [5]. At large enough R , a denser (heavier) gas is located above an underdense (lighter) gas. This drives thermal convection: a small sinusoidal perturbation in the horizontal direction grows if the relative heat loss parameter R exceeds a critical value that depends on F , K and the horizontal wave number.

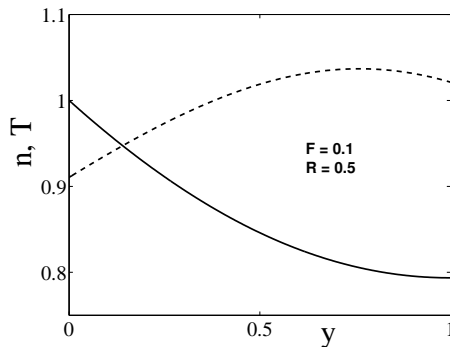


FIG. 1: Static temperature (solid line) and density (dashed line) profiles for $F = 0.1$ and $R = 0.5$.

The linear stability analysis involves linearization of Eqs. (1)–(3) around the static solutions $n_s(y)$ and $T_s(y)$. The linearized equations are

$$\frac{\partial n}{\partial t} + n_s \frac{\partial v_x}{\partial x} + \frac{\partial}{\partial y} (n_s v_y) = 0; \quad (6)$$

$$n_s \frac{\partial v}{\partial t} = -r (n_s T + T_s n) + \frac{1}{2} K r \left(\frac{\partial^2 \hat{D}}{\partial x^2} \right) - F n_s; \quad (7)$$

$$n_s \frac{\partial T}{\partial t} + T_s^0 v_y + n_s T_s r = -K r^2 (T_s^{1=2} T) - K R T_s^2 T_s^{3=2} \frac{2n}{n_s} + \frac{3T}{2T_s}; \quad (8)$$

where n , T and v denote small perturbations. Exploiting the symmetry of the static state in the horizontal direction, we can consider a single Fourier mode:

$$\begin{aligned} n(x; y; t) &= e^{-t} N(y) \cos k_x x; \\ T(x; y; t) &= e^{-t} T(y) \cos k_x x; \\ v_x(x; y; t) &= e^{-t} u(y) \sin k_x x; \\ v_y(x; y; t) &= e^{-t} v(y) \cos k_x x; \end{aligned} \quad (9)$$

where λ is the scaled growth/decay rate, and k_x is the scaled horizontal wave number. Substituting Eq. (9) into Eqs. (6)–(8) and eliminating N , we obtain three homogeneous ordinary differential equations that can be written as a single equation for the eigenvector $U(y) = [T(y); u(y); v(y)]$, corresponding to the eigenvalue λ :

$$A U'' + B U' + C U = 0; \quad (10)$$

where

$$A = \begin{pmatrix} 0 & 0 & 0 & 1 \\ K a_0 & 0 & 0 & 0 \\ 0 & K a_0 = 4 & 0 & 0 \\ 0 & 0 & K a_0 = 4 & n_s T_s = \end{pmatrix} A; \quad (11)$$

$$B = \begin{pmatrix} 0 & 0 & 0 & 1 \\ 2K a_1 & 0 & 2K R T_s^2 T_s^{3=2} & n_s T_s \\ 0 & K a_1 = 4 & k_x n_s T_s = & 0 \\ n_s & k_x n_s T_s = & K a_1 = 4 & T_s n_s^0 = \end{pmatrix} A; \quad (12)$$

while the elements of matrix C are

$$\begin{aligned} C_{11} &= K a_2 - 3K R T_s^2 a_0 = 2 - K k_x^2 a_0 + n_s; \\ C_{12} &= 2K R T_s^2 T_s^{3=2} k_x = k_x n_s T_s; \\ C_{13} &= 2K R n_s T_s^{3=2} n_s^0 = n_s T_s^0; \\ C_{21} &= k_x n_s; \\ C_{22} &= k_x^2 n_s T_s = + n_s - K k_x^2 a_0 = 4; \\ C_{23} &= k_x T_s n_s^0 = K k_x a_1 = 4; \\ C_{31} &= n_s^0; \\ C_{32} &= K k_x a_1 = 4; \\ C_{33} &= (T_s^0 n_s + T_s n_s^0) = + n_s - K k_x^2 a_0 = 4; \end{aligned} \quad (13)$$

We have denoted for brevity $a_0 = T_s^{1=2}(y)$; $a_1 = a_0^0$ and $a_2 = a_0^0$. The BCs for the functions T , u and v are the following:

$$T(0) = T(1) = u(0) = u(1) = v(0) = v(1) = 0; \quad (14)$$

Equation (10) with the BCs (14) define a linear boundary-value problem: there are three BCs at the base and three at the top. A simple numerical procedure (realized in MATLAB) enabled us to avoid the unpleasant shooting in three parameters. The procedure employs the linearity of the problem. We first complement the three BCs at the base by three arbitrary BCs, and compute numerically three independent solutions of Eqs. (10). The general solution can be represented as a linear combination of these three independent solutions that includes three arbitrary coefficients. Demanding that the three BCs at the top be satisfied, we obtain three homogeneous linear algebraic equations for the coefficients. A nontrivial solution demands that the determinant vanish, which yields the eigenvalue. Varying R at fixed F , K and k_x , we determine the critical value $R = R_c$ for instability from the condition $\text{Re} \sigma = 0$.

In the whole region of the parameter space that we explored we found that $\text{Im} \sigma = 0$ at the instability onset. Therefore, thermal granular convection does not exhibit overstability and can be analyzed in terms of marginal stability. Figure 2a shows the marginal stability curves versus the horizontal wave number k_x at a fixed K and two different values of F . The curves exhibit minima at $(k_x; R_c)$, similarly to the convection in classical fluids [7]. Therefore, the convection threshold in the horizontally infinite layer is $R = R_c$. Close to the onset, the expected horizontal size of the convection cell is $2\pi/k_x$. Figure 3 depicts the convection cells obtained by plotting the field lines of the respective velocity field, found numerically, at the onset. One can see that at small F the cells typically occupy the whole layer and are elongated in the horizontal direction. At large F the cells are much smaller, located near the base, and their aspect ratio is close to unity.

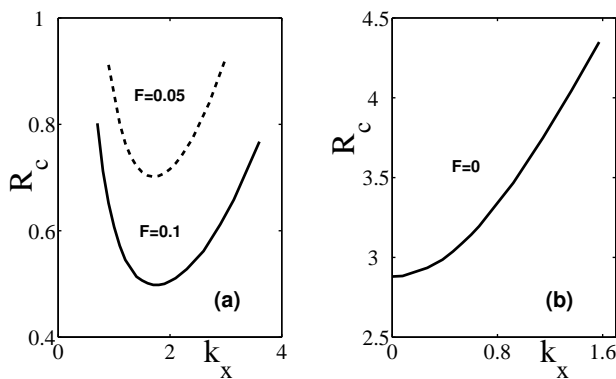


FIG. 2: The critical values of the relative heat loss parameter R for the convection instability (a non-zero gravity, a) and phase-separation instability (zero gravity, b) versus the horizontal wave number k_x . The Knudsen number $K = 0.02$.

Figure 2b corresponds to a zero gravity: $F = 0$. Here a different symmetry-breaking instability occurs: the one that leads to phase separation [15, 16, 17, 18, 19, 20].

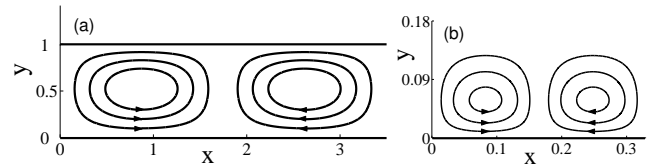


FIG. 3: Convection cells at the instability onset $k = k_x$ and $R = R_c$. The Knudsen number is $K = 0.02$. Figure a corresponds to the solid curve of Fig. 2a. Here $F = 0.1$, $k_x = 1.8$ and $R_c = 0.49$. Figure b corresponds to the large- F limit, when the granulate is localized near the base. Here $F = 5$, $k_x = 19$, and $R_c = 2.86$.

When R exceeds the marginal stability threshold R_c ($F = 0$), the laterally symmetric stripe of enhanced particle density at the top wall becomes unstable and gives way to a 2D steady state. In contrast to convection, this 2D steady state is static: no macroscopic flow. R_c ($F = 0$) can be calculated analytically [16]. In our present notation, it is determined from the algebraic equation $\coth \eta = \eta$, where $\eta = (R_c/2)^{1/2}$. This yields R_c ($F = 0$) = 2.8785... The minimum of the marginal stability curve occurs here at $k_x = 0$, that is for an infinitely long wavelength.

We found that the crossover between the two instabilities is continuous. The dependences of R_c and k_x on the Froude number F are shown in Fig. 4. One can see that R_c (F) dependence is non-monotonic. A stronger gravity is favorable for convection at very small F (as Fig. 2a also shows). However, this tendency is reversed at $F \approx 0.16$, and R_c starts to grow with F until it saturates at large F . In its turn, k_x goes down monotonically with F and vanishes at $F = 0$. The decrease is quite slow at intermediate F , but becomes very rapid at very small F . As the phase separation instability does not exist in classical fluid, this low- F behavior is unique for granular fluid.

The large- F limit deserves a special attention. Here the granulate is localized near the base. This regime is convenient in experiment, as particle collisions with the top wall (which are in reality inelastic) are avoided. A natural unit of distance in this regime is $\lambda = T_0/mg$, while the time should be scaled to $\tau = T_0^{1/2}$. Correspondingly, $h\eta$ is defined now as the number of particles per unit length in the horizontal direction, divided by λ . After rescaling, one can see that the Froude number F drops out of Eqs. (1)–(3) and enters the problem only through the layer height that becomes $H = \lambda = F$. For $F \gg 1$ the top wall can be safely moved to infinity, and F drops out of the problem completely. Therefore, at large F , the convection threshold R_c should depend only on K , and be independent of F . Our numerical results support this prediction, see Fig. 4a. How should k_x behave at large F ? Let us reintroduce for a moment the "physical" (dimensional) horizontal wave number $k_{x,ph}$. The scaled critical wave number $k_x = k_{x,ph} H = k_{x,ph} F$. As the

product $k_{x,ph}$ is the scaled wave number in the newly rescaled variables, it should be independent of F at large F . Therefore, k_x should be proportional to F . Figure 4b shows that the quantity k_x/F indeed approaches a constant (that depends on K) at large F .

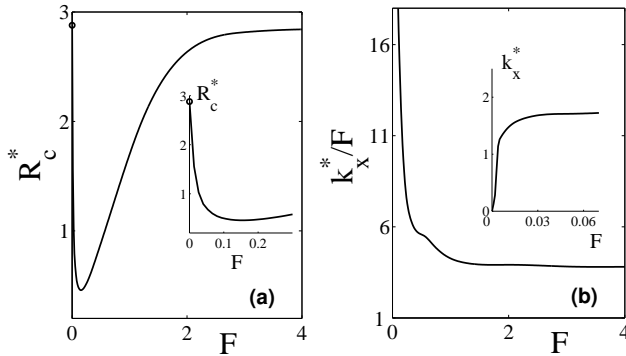


FIG. 4: Convection threshold versus the Froude number F . Shown are the $R_c(F)$ (a) and $k_x(F)$ (b) dependences at $K = 0.02$. The insets show that $R_c \rightarrow 2.8785$ and $k_x \rightarrow 0$ as $F \rightarrow 0$. For large F , the quantity $R_c \rightarrow 2.85$ (a), while $k_x/F \rightarrow 3.80$ (b).

The dependence of the convection threshold R_c on the Knudsen number K (at a fixed F) is shown in Fig. 5. R_c should grow with K because the viscosity and heat conduction (both of which scale like K) tend to suppress convection [5]. As $K \rightarrow 0$ they become negligible. One should still expect a non-zero R_c here (see Fig. 5), similarly to classical fluids, where the Rayleigh criterion (or, rather, its generalization to compressible fluid [8, 9, 10, 11]) gives way to the Schwarzschild criterion [7] that is independent of the transport coefficients.

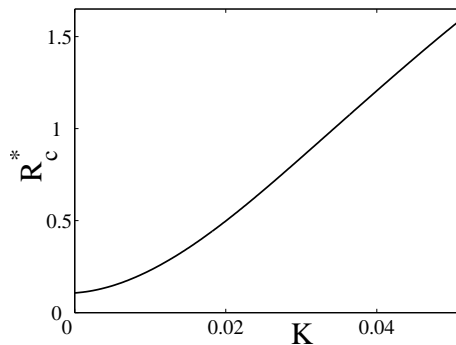


FIG. 5: Convection threshold R_c versus the Knudsen number K at $F = 0.1$. R_c is non-zero at $K \rightarrow 0$.

In summary, we employed the hydrodynamic model [5] for a linear stability analysis of the static state in an infinite horizontal layer of granular gas driven from below. The theory should be valid when the mean free path of the particles is much smaller than any length scale described hydrodynamically. We found the convec-

tion threshold, in terms of the relative heat loss number R , versus the two other scaled numbers: the Froude number F and the Knudsen number K . We predicted the morphology of convection cells at the onset of convection. As $F \rightarrow 0$, the convection instability goes over continuously into the phase-separation instability [15, 16, 17, 18, 19, 20]. At large F , a universal limit is reached, when the convection threshold depends only on K . Further developments of the theory should account for the excluded-volume effects [12] that have been shown to be important in the limit of $F \rightarrow 0$ [15, 16, 17, 18, 19].

We gratefully acknowledge useful discussions with Igor S. Aranson, John M. Finn, Xiaoyi He, Pavel V. Sasorov and Victor Steinberg. The work was supported by the Israel Science Foundation administered by the Israel Academy of Sciences and Humanities.

-
- [1] G.H. Rislow, *Pattern Formation in Granular Materials*, (Springer, Berlin, 2000).
 - [2] R. Ramirez, D. Risso, and P. Cordero, *Phys. Rev. Lett.* 85, 1230 (2000).
 - [3] R.D. Wildman, J.M. Huntley, and D.J. Parker, *Phys. Rev. Lett.* 86, 3304 (2001).
 - [4] P. Sunthar and V. Kumaran, *Phys. Rev. E* 64, 041303, (2001).
 - [5] X. He, B. Meerson, and G. Doolen, *Phys. Rev. E* 65, 030301(R) (2002).
 - [6] J. Talbot and P. Viot, *Phys. Rev. Lett.* 89, 064301 (2002).
 - [7] S. Chandrasekhar, *Hydrodynamics and Hydrodynamic Stability* (Dover, New York, 1981).
 - [8] E.A. Spiegel, *Astrophys. J.* 141, 1068 (1965).
 - [9] M.S. Gitterman and V.A. Steinberg, *High Temp.* 8, 754 (1970); *J. Appl. Math. Mech.* 34, 305 (1971).
 - [10] M.S. Gitterman, *Rev. Mod. Phys.* 50, 85 (1978).
 - [11] P. Carles and B. Ugurtas, *Physica D* 126, 69 (1999).
 - [12] J.T. Jenkins and M.W. Richmond, *Phys. Fluids* 28, 3485 (1985).
 - [13] J.J. Brey and D. Cubero, in *Granular Gases*, edited by T. Poschel and S. Luding (Springer, Berlin, 2001), pp. 59-78; I. Goldhirsch, *ibid.*, pp. 79-99.
 - [14] M.C. Cross and P.C. Hohenberg, *Rev. Mod. Phys.* 65, 851 (1993); E. Bodenschatz, W. Pesch and G. Ahlers, *Annu. Rev. Fluid. Mech.* 32, 709 (2000).
 - [15] E. Lvne, B. Meerson, and P.V. Sasorov, *cond-mat/008301*; *Phys. Rev. E* 65, 021302 (2002).
 - [16] E. Khaïn and B. Meerson, *cond-mat/0201569*; *Phys. Rev. E* 66, 0213XX (2002).
 - [17] E. Lvne, B. Meerson, and P.V. Sasorov, *cond-mat/0204266*.
 - [18] M. A. Argentea, M.G. Clerc, and R. Soto, *Phys. Rev. Lett.* 89, 044301 (2002).
 - [19] E. Khaïn and B. Meerson, *Phys. Rev. Lett.* (submitted).
 - [20] B. Meerson, T. Poschel, P.V. Sasorov, and T. Schwager, *cond-mat/0208286*.